Journal of the Serbian Chemical Society
JSCS-info@shd.org.rs • www.shd.org.rs/JSCS
J. Serb. Chem. Soc. 78 (12) 2053–2067 (2013)
JSCS–4550
UDC 669.14.018.8+546.3–31:
621.315.59+620.193:539.216
Original scientific paper

Change of *n*-type to *p*-type conductivity of the semiconductor passive film on N-steel: Enhancement of the pitting corrosion resistance

MIRJANA METIKOŠ-HUKOVIĆ[1]*, ZORAN GRUBAČ[2] and SASHA OMANOVIC[3]

[1]Department of Electrochemistry, Faculty of Chemical Engineering and Technology, University of Zagreb, P. O. Box 177, 10000 Zagreb, Croatia, [2]Department of General and Inorganic Chemistry, Faculty of Chemistry and Technology, University of Split, N. Tesle 10, 21000 Split, Croatia and [3]Department of Chemical Engineering, McGill University, 3610 University Street, Montreal, Quebec, Canada H3A 2B2

(Received 21 November, revised 24 November 2013)

Abstract: Electrochemically-assisted modification of the surface of N-austenitic stainless steel (ASS N25) was successfully employed to improve the barrier properties of the passive film in a chloride-containing solution. The chemical composition, electronic and barrier properties of the surface film before and after the electrochemical treatment were examined using X-ray photoelectron spectroscopy (XPS) and electrochemical impedance spectroscopy (EIS). The electrochemical measurements were performed in a corrosion testing solution. The excellent corrosion resistance (both pitting and general) of the modified surface of the N-steel was discussed according to a Mott–Schottky analysis of the interfacial capacitance of the space charge layer and EIS results. The conductivity change of the surface film from an *n*- to a *p*-type in the pitting susceptible region was explained using the XPS analysis and the semiconducting properties of the film.

Keywords: stainless steel; corrosion; passive films; metal oxide semiconductors.

INTRODUCTION

It was reported that the favourable effect of nitrogen on the electrochemical and mechanical properties of austenitic stainless steels (ASS) is a consequence of the electronic exchange between the iron and nitrogen atoms in austenitic fcc lattice, in which nitrogen contributes to the electronic states just at the Fermi level.[1] According to these authors, the increase in the free electron density due to

* Corresponding author. E-mail: mmetik@fkit.hr
doi: 10.2298/JSC131121144M

the nitrogen atoms in the iron lattice favours short-range ordering and enhances the metallic character of the interatomic bonds. Bonding between atoms of non-identical elements results in an enhanced thermodynamic stability of a solid solution, and thus much better corrosion and mechanical properties. Austenitic stainless steels (SSs) with nitrogen (ASS N25) offer acceptable resistance against general corrosion in a variety of corrosive environments.[2–4] Nitrogen is believed to play a major role pertaining to the corrosion properties of austenitic stainless steels, as it promotes passivity, and enhances the re-passivation properties of the stainless steel, in addition to its contribution to the mechanical strength.[5,6]

Although the improved corrosion resistance of nitrogen-containing SSs justifies their employment in many applications, the related literature indicates that vigorous pitting attacks still prevail when these SSs are exposed to chloride-containing solutions.[6] This evidences insufficiency in the improvement of the corrosion protection brought about by nitrogen addition to the stainless steel. Pitting attacks are not only responsible, to a large extent, for the mechanical failure of SSs, mainly in industrial applications, but also cause the release of bio-hazardous species into the surrounding environments, which are of particular concerns in food, pharmaceutical and biomedical applications.[7,8]

The pitting resistance of SSs is directly linked to the stability of the surface passive film, and is thus dictated by its physico-chemical properties. Oxide passive films grown on metal and alloy surfaces have recently been reviewed[9–11] and recent insights into the mechanism of passivity breakdown and localized (pitting) corrosion were given.[12,13] It was established that during passive film formation/growth on an ASS N25 electrode, Fe^{3+} species migrate outward through the cation vacancies ($V_{Cr^{3-}}$, are the main charge carriers) in the Cr_2O_3 layer.[14] Thus, the passive film on ASS N25 is believed to be comprised of an inner Cr_2O_3 barrier layer and an outer iron-rich sublayer,[15] whereby the point defect model (PDM) best explains the kinetics of passive film growth.[16,17]

Numerous efforts have been made to modify the structure of passive films and thus enhance the pitting and general corrosion resistance of stainless steels. The outcome ranged from very poor success to remarkable improvements in the properties of the passive films.[18–22]

Cyclic potentiodynamic polarization, as a surface treatment method, has been reported as an efficient method that could be employed to modify the physicochemical and electronic properties of the passive films on 316LVM stainless steel.[23,24]

In this paper, the effect of cyclic potentiodynamic polarization on the corrosion resistance of ASS N25 surface is presented. The pitting and barrier properties of an unmodified and a modified ASS N25 surface are also comparatively discussed based on the semiconducting properties of naturally and electrochemically grown passive films.

EXPERIMENTAL

A single compartment standard electrochemical cell was used in all electrochemical/corrosion measurements. The reference electrode (RE) was a saturated calomel electrode (SCE), and a platinum plate was used as the counter electrode (CE). A working electrode (WE) was made of ASS N25 samples with the chemical composition given in Table I. The WE was prepared by cutting ASS N25 into disc-shaped samples suitable for the EG&G PAR flat specimen holder, model K105. The sample area exposed to an electrolyte was 0.785 cm^2. All current density values reported in this work were normalized with respect to this geometrical surface area. Electrochemical passivation of the electrode surface was performed in a 0.1 M $NaNO_3$ solution. Corrosion tests were realized in a 0.16 M NaCl solution.

TABLE I. Chemical composition (mass %) of ASS N25 steel (the balance is Fe)

C	Mn	Si	Cr	Ni	Mo	N	Nb
0.030	4.60	0.29	21.15	12.72	2.22	0.247	0.170

The composition of the passive films was determined by X-ray photoelectron spectroscopy (XPS). The XPS spectra were recorded in a UHV chamber of a SPECS system with a Phoibos MCD 100 electron analyzer and monochromatised Al K_λ X-rays of 1486.74 eV. For the pass energy of 10 eV used in the present study, the total energy resolution was around 0.8 eV. The photoemission spectra were simulated with several sets of mixed Gaussian–Lorentzian functions with Shirley background subtraction.

In order to measure the surface corrosion resistance, electrode stabilization at the open circuit potential (OCP) was first performed in the corrosion testing solution for one hour. Next, electrochemical impedance spectroscopy (EIS) measurement was performed at the OCP in a frequency range between 100 kHz and 30 mHz with an *ac* amplitude (rms) of ±10 mV. Pitting polarization experiments were conducted by anodically polarizing the working electrode (WE) from 50 mV negative of the OCP to the potential at which the current density of 1 mA cm^{-2} was reached. Chronoamperometry measurements were performed following electrode stabilization at the OCP in a corrosion testing solution by potentiostatically (constant potential) polarizing the WE and measuring the resulting current density.

To investigate the semiconducting properties of naturally-grown (unmodified surface) and electrochemically formed passive films, capacitance measurements were performed in a borate buffer solution, pH 8.4 under a cathodic bias, starting from 1.0 V down to –0.9 V. The imaginary part of the impedance (Z_{imag}) measured at the frequency of 1.6 kHz was recorded as a function of the potential. The applied *ac* amplitude was ±10 mV. The experimental setup consisted of a PAR 273A potentiostat/galvanostat for voltammetric measurements, and a Solartron SI 1287 potentiostat/galvanostat and a Solartron SI 1255 HF frequency response analyzer for the electrochemical impedance spectroscopy measurements.

RESULTS AND DISCUSSION

Electrochemical formation of passive films on an ASS N25 surface

The cyclic voltammograms (CV) of an ASS N25 electrode recorded in a 0.1 M $NaNO_3$ in the potential region between –0.8 V and 0.9 V, representing the 1st (solid line) and the 300th (dashed line) sweeps, are shown in Fig. 1. It is evident that the shape of the CV changed significantly with the number of polarization sweeps. The anodic and cathodic shoulders/peaks observed on the voltammo-

grams and their corresponding redox reactions have already been explained in the literature,[25–29] and will not be elaborated in detail here. Briefly, in each sweep two oxidation reactions, Fe → Fe(II)/Fe(III) and Cr(III) → Cr(VI) in the anodic sweep, and their corresponding reduction reactions in the cathodic sweep, occur.[23] The first anodic shoulder/peak (at *ca.* –0.7 V) is related to the formation of a Fe(II)/Fe(III)-oxide layer (*i.e.*, Fe_2O_3) on the top of the Cr(III) oxide layer, followed by oxidation of the Cr(III) species to soluble Cr(VI) species (at *ca.* –0.1 V). The corresponding reduction reactions in the reverse sweep occur at potentials negative of *ca.* –0.4 V.

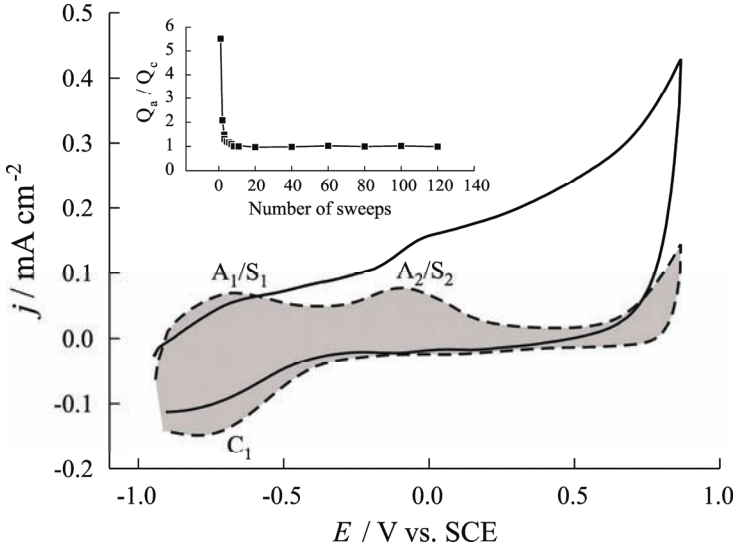

Fig. 1. Cyclic voltammograms of the freshly polished ASS N25 surface recorded in a 0.1 M $NaNO_3$ solution at a scan rate of 0.167 mV s^{-1}. The solid line represents the 1st sweep, and the broken line represents the 300th sweep. Inset: dependence of the anodic to cathodic total charge ratio on the number of sweeps.

On the freshly polished ASS N25 surface (1st sweep), the anodically formed Cr(VI)-species are mainly dissolved in the solution by diffusion through a very thin and non-compact pre-formed passive film. This explains the absence of a passive transition associated with the oxidation of Cr(III) to Cr(VI) in the anodic scan (shoulder S_2). On the other hand, the 300th sweep in Fig. 1 shows that the charge associated with the Cr(III)-to-Cr(VI) transition in the potential region of Cr(III) oxidation (positive of *ca.* –0.4 V) is negligible compared to that recorded in the first sweep. This demonstrates that the Cr(VI) species formed in the anodic sweep remain "locked" in the surface passive film. The results in Fig. 1 suggest that the passive film formed during prolonged cyclization of the electrode is more

compact or thicker than the film formed in the 1st sweep; thus effectively preventing the dissolution of Cr(VI) species into the electrolyte.

In order to obtain a better quantitative insight into changes during the cyclization of the ASS N25 electrode, the ratio of the total anodic-to-cathodic charge is presented as an inset to Fig. 1. The curve shows that the anodic reactions in the 1st sweep are quite irreversible ($Q_a/Q_c \approx 5.5$) and that only *ca.* 18 % of the charge related to these anodic processes is used to form species that do not dissolve into the solution but form the surface passive oxide film. However, on cyclization of the surface, the reversibility of the anodic processes rapidly increases, and after *ca.* 10 sweeps it approaches almost 100 %. This indicates that the cyclic polarization of the working electrode surface under the given conditions significantly enhances passivity of the surface oxide film, preventing the dissolution of the underlying metals into the solution, even at high anodic potentials. Similar behaviour was shown in the case of 316LVM stainless steel, when a considerable improvement in the corrosion resistance was observed.[24,25]

Chemical composition of passive films formed on an ASS N25 electrode – XPS characterization

The chemical composition of the electrochemically modified passive film and the naturally grown passive film (unmodified surface) was analyzed by XPS. The photoemission spectra (open circles) around the Cr $2p_{3/2}$ and Fe $2p_{3/2}$ energy levels recorded on an a) unmodified and b) electrochemically modified sample are shown in Fig. 2, together with the numerical fits (solid lines) obtained using Voigt profiles. The agreement between the modelled and experimental data is very good.

A comparison of the corresponding spectra revealed that Cr(VI) species were detected only in the electrochemically formed passive film. Chromium in both passive films was found as Cr(III) in $Cr(OH)_3$ and in Cr_2O_3. Both passive films contain Fe(II) and Fe(III), mostly in Fe_3O_4, with some contribution of Fe(II) in FeO. The peaks at 715.3 and 713.4 eV are well-known shake-up satellite peaks. Iron oxide satellite structures are frequently used as fingerprints to identify the iron oxide phases. The shake-up satellite in Fig. 2 at 715.3 eV can be assigned to Fe(II) in FeO, while the other satellite peak at 713.4 eV is attributed to Fe(II) in chromite ($FeCr_2O_7$). No shake-up satellite structures are visible on the chromium spectra.

Corrosion resistance of passive films formed on ASS N25 surfaces

Polarization voltammograms of the unmodified ASS N25 surface (solid line) and surfaces modified electrochemically (broken lines), recorded in 0.16 M NaCl solution, are shown in Fig. 3. The polarization curve of the unmodified surface

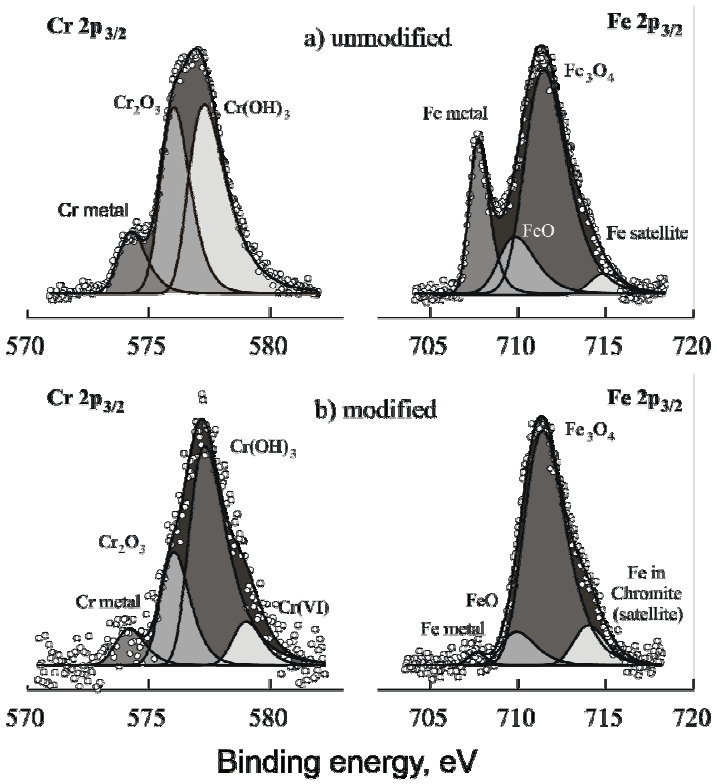

Fig. 2. The deconvoluted XPS spectra of Cr $2p_{3/2}$ and Fe $2p_{3/2}$ energy levels obtained for: a) an unmodified and b) an electrochemically modified ASS N25 surface.

exhibits a number of current spikes at potentials below 0.4 V, indicating the formation of metastable pits in this potential region. However, the formation of stable pits occurs at potentials positive of 0.4 V, which is in agreement with the results for austenitic types of stainless steels.[26,27] However, at potentials higher than *ca.* 0.5 V, the current density starts to rise more steeply and finally at more noble potentials, a breakdown of the film occurs. In the reverse scan, a pitting loop appears. On the other hand, the response of the electrochemically modified surfaces shows the absence of current spikes. An abrupt increase in anodic current at *ca*. 1.2 V could be connected with the oxygen evolution reaction. Moreover, the passive current density of these surfaces is significantly lower than that of the unmodified surface. With increasing number of passivation sweeps (from 50 to 200 scans), the passive current decreases, thus confirming that a more compact and the corrosion resistant surface film had been formed after a higher number of passivation scans. In summary, the results in Fig. 3 evidence that the electrochemical passivation of the ASS N25 surface improves its pitting corrosion resistance and passivity in a 0.16 M NaCl solution.

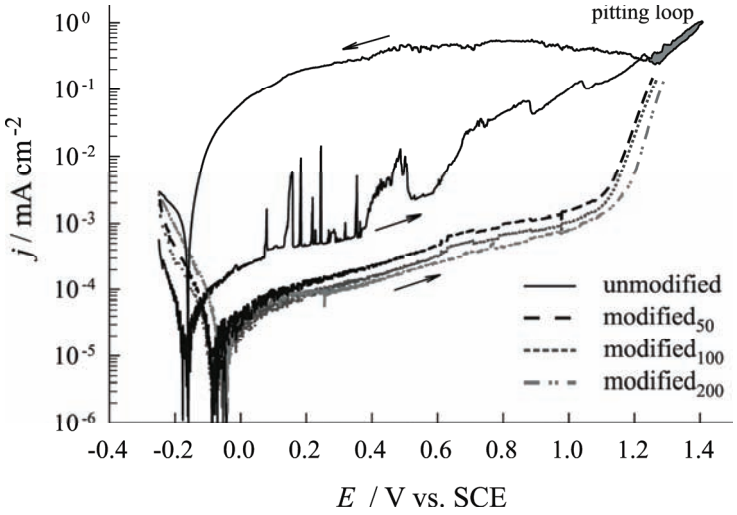

Fig. 3. Tafel plots of the polarization curves of the unmodified (solid line) and the electrochemically modified ASS N25 surface recorded in a 0.16 M NaCl solution at a scan rate of 0.167 mV s^{-1}. Modification of the surface was realised by applying 50 sweeps (broken line), 100 sweeps (dotted line) and 200 sweeps (dash dot dot dash line).

Investigation of the frequency of the formation of metastable pits under potentiostatic polarization, in the pitting susceptible region, is another criterion used to evaluate surface resistance against pitting corrosion. In other words, the higher the density of pitting-active spots on the surface, the higher is the susceptibility of the surface to pitting corrosion. On a current–time curve, recorded at a selected potential in the pitting-susceptible region, this is manifested as the appearance of current spikes. The chronoamperometry (CA) plots of the unmodified (1), and electrochemically modified (2) surfaces are comparatively shown in Fig. 4. The CA plot of the unmodified surface clearly shows the incidence of pitting corrosion, evidenced by the continuous and "rough" increase in current with time. On the other hand, the response of the electrochemically passivated surface is characterized by a “zero” line. Hence, the results presented in Fig. 4 clearly support the conclusions made from the results presented in Fig. 3, suggesting that the electrochemical passivation of ASS N25 yielded a passive film with excellent corrosion protection properties.

Semiconducting properties of the passive films formed on an ASS N25 surface

Correlation between the semiconducting properties of passive oxide films and their resistance against pitting corrosion was reported in the literature.[28–30] The semiconducting (electronic) properties of passive films have generally been studied using capacitance measurements, employing the Mott–Schottky analysis:[31]

$$\frac{1}{C_{SC}^2} = \frac{-2}{\varepsilon\varepsilon_0 e N_A}\left(E - E_{fb} - \frac{kT}{e}\right) \quad (1)$$

$$\frac{1}{C_{SC}^2} = \frac{2}{\varepsilon\varepsilon_0 e N_D}\left(E - E_{fb} - \frac{kT}{e}\right) \quad (2)$$

where ε is the relative permittivity (dielectric constant) of the oxide film, ε_0 is the vacuum permittivity (F cm^{-1}), e is the elementary charge of an electron (C), N_A is the acceptor density (cm^{-3}) and N_D is the donor density (cm^{-3}) in the non-stoichiometric passive film, E_{fb} is the flat-band potential (V), k is the Boltzmann constant (J K^{-1}) and T is the temperature (K).

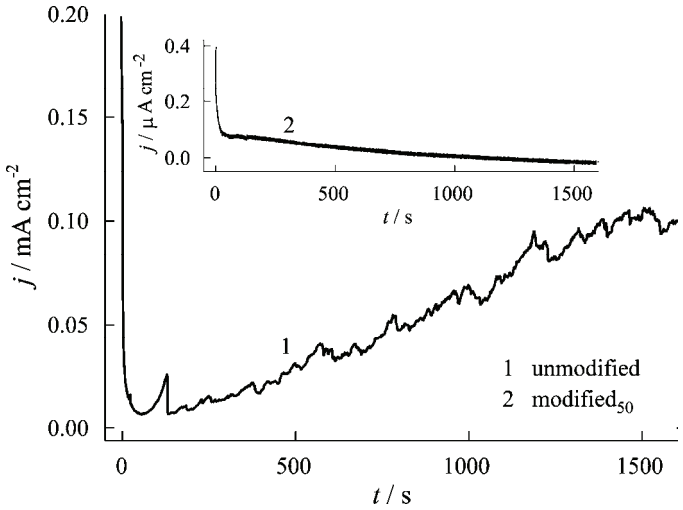

Fig. 4. Potentiostatic curves of the unmodified (1) and the electrochemically modified (2) ASS N25 surfaces recorded in a 0.16 M NaCl solution at a potential 0.45 V. Modification of the surface was realised by applying 200 sweeps.

The passive film/electrolyte interface is, in this analysis, treated as the space charge depletion zone, which behaves as a Schottky barrier. Thus, the measured capacitance, after correction for the electrochemical double layer capacitance, is attributed to the space charge capacitance, C_{SC}, inside the oxide film. If an oxide film behaves as a semiconductor that can be described by the Mott–Schottky model, the dependence between $1/C_{SC}^2$ *vs.* E should give a straight line. For an *n*-type semiconductor, the equation has a negative slope, while for a *p*-type semiconductor, the equation has a positive slope.

The Mott–Schottky response of a naturally grown passive film (unmodified surface) and of the passive film formed by applying a specific number of polarization (modification) cycles (Fig. 5) shows the existence of several potential regions characterizing the semiconducting behaviour of the corresponding sur-

face films. In the potential region between –0.9 and –0.6 V (Region I), the passive films behave as *p*-type semiconductors, while in the potential range between –0.3 and 0 V or 0.2 V for the unmodified and modified surface, respectively, (Region II), *n*-type behaviour is clearly visible. An *n*-type behaviour has been correlated with the response of iron oxides in the passive film, which are characterized by a non-stoichiometric composition resulting in oxygen vacancies that contribute to the *n*-type conductivity.[4,15,32,33] On the other hand *p*-type behaviour has been attributed to the response of chromium oxides, and is characterrized by the non-stoichiometry resulting in metal vacancies that contribute to the *p*-type semiconductivity.[4,15,34–36] Taking this into account, it could be concluded that in Region I, the space charge depletion zone is situated in the part of the passive film that is reach by chromium(III) oxide and behaves as a Schottky barrier, while the remaining Fe oxide rich part of the oxide is in a condition of accumulation. On the other hand, at potentials in Region II, the semiconducting property of the passive film is determined by the space charge depletion zone located in the iron oxide rich layer, while the chromium(III) oxide rich layer is in the accumulation condition.[32] In Region IV (at $E > 0.8$ V and $E > 1.2$ V), due to ionic (pitting corrosion) and electronic (oxygen evolution) transfer reactions on the solid/electrolyte interface, the main potential drop is no longer in the space charge layer but in the Helmholtz layer.

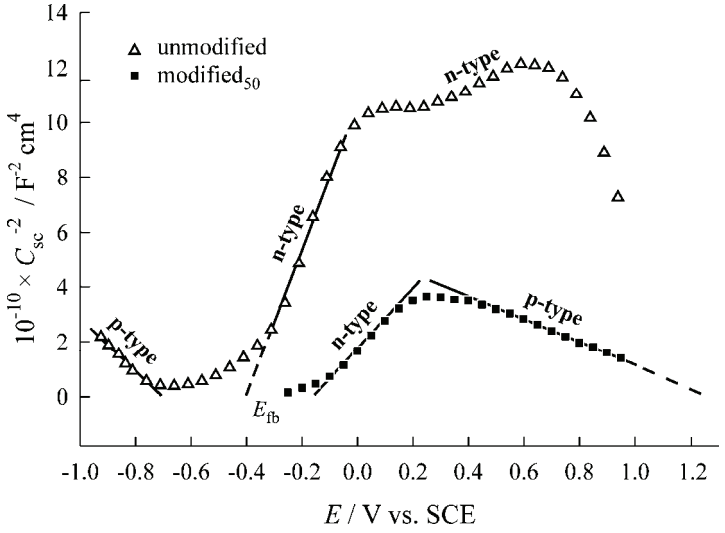

Fig, 5. Mott–Schottky plot of the unmodified (Δ) and the electrochemically modified (■) ASS N25 surfaces by applying 50 sweeps.

The main difference in $1/C_{SC}^2$ *vs.* E behaviour between the unmodified and the electrochemically modified surface is in Region III (0.2–0.7 V), in which the two surfaces display different types of semiconductivity. Here, focus will be

directed only to this region since it coincides with the pitting potential region of the unmodified surface (Fig. 3). Figure 5 shows that the unmodified surface behaves as an *n*-type semiconductor in Region III. There is general agreement that surfaces presenting *n*-type semiconductivity are more prone to pitting compared to surfaces exhibiting *p*-type semiconductivity.[28]

If the Mott–Schottky plot (Fig. 5) and the polarization curve (Fig. 3) of the unmodified sample are compared, it will be seen that the pitting potential coincides well with the *n*-type behaviour in Region III. This is quite in agreement with the point defect theory (PDM),[16,17] which states that the initial pitting reaction that occurs at a film/solution interface involves the adsorption of chloride ions into oxygen vacancies according to relation:

$$V_{O}^{\bullet\bullet}(\text{ox}) + \text{Cl}^{-} \cdot \text{n H}_2\text{O} \rightarrow V_{\text{Cl}}^{\bullet}(\text{ox}) + \text{n H}_2\text{O} \quad (3)$$

where $V_{O}^{\bullet\bullet}(\text{ox})$ is the positively charged oxygen vacancy, Cl^{-} is the chloride ion in an aqueous electrolyte and $V_{\text{Cl}}^{\bullet}(\text{ox})$ is the chloride vacancy occupying an oxygen lattice site (Kröger–Vink notation). To preserve electroneutrality, an equivalent number of cation vacancies, V_{M}^{3-}, must be formed through a corrosion process of metal dissolution.

Taking into account the PDM, it is assumed that an increase in the pitting corrosion resistance of a material could be achieved by increasing the concentration of metal vacancies in the passive film. This process occurs by the cyclic potentiodynamic formation of the passive film under the conditions presented in Fig. 1. Namely, by polarizing the ASS N25 surface (between the potentials of hydrogen and oxygen evolution) at high anodic potentials, Cr(VI) species are formed (see XPS results presented in Fig. 2). With cyclization, progressively more of these species remain "arrested" in the growing passive film. The formation of Cr(VI) species increases the oxygen content in the passive film (so-called secondary passivity), producing an increase in the density of metal vacancies, V_{M}^{3-}, according to the equation:[14]

$$\text{Cr(III)} \rightarrow \text{Cr(VI)} + V_{M}^{3-} + 3e^{-} \quad (4)$$

Electrochemical modification, in turn, leads to the changes in the electronic properties of the surface film and to the increased pitting resistance (Figs. 3 and 4). On the Mott–Schottky plot (Fig. 5), in the pitting susceptible Region III, a transition from *n*- to *p*-type conductivity occurs. Mott–Schottky results for the flat band potentials and charge carrier densities of the unmodified and modified film are summarized as follows:

i) unmodified surface of the steel: $E_{\text{fb}} = -0.405$ V, $N_{\text{D}}(\text{Fe}_2\text{O}_3) = 3.95\times10^{19}$ cm^{-3};

ii) modified surface of the steel: $E_{\text{fb}} = -0.179$ V, $N_{\text{D}}(\text{Fe}_2\text{O}_3) = 1.30\times10^{20}$ cm^{-3} and $E_{\text{fb}} = 1.250$V, $N_{\text{A}}(\text{CrO}_3) = 3.54\times10^{20}$ cm^{-3}.

The values obtained for the donor and acceptor densities were of the same order of magnitude as those reported previously for ASSs, without nitrogen.[32,35,37,38]

Barrier properties of the passive films formed on ASS N25 surfaces

In order to investigate the general corrosion resistance of the electrochemically modified ASS N25 surfaces, EIS measurements were performed and presented as the Nyquist plots in Fig. 6. To better investigate the frequency-dependent processes occurring at the surface/electrolyte interface and inside the passive oxide films, the EIS data were modelled using nonlinear least-squares fit analysis.[39] An equivalent electrical circuit (EEC) presented in the inset to Fig. 6 was used to model the experimental data presented in Fig. 6. R_{el} represents the electrolyte resistance, CPE is a constant phase element representing a double-layer capacitance, R_1 is the corrosion resistance and C_0 can be attributed to the faradaic pseudocapacitance corresponding to the film thickness/potential variation.[40–42] The values obtained by fitting the experimental EIS data using the presented EEC are given in Table II. It should be noted that the values presented in Table II were recorded for ASS N25 surfaces prior to the pitting polarization tests.

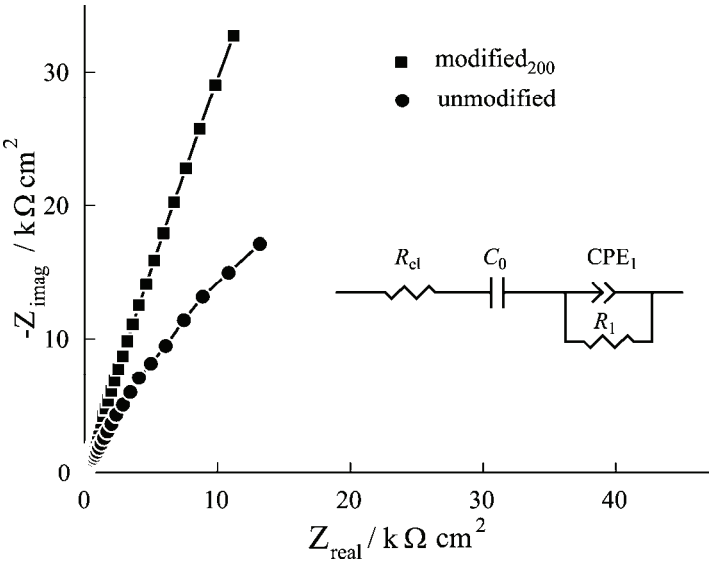

Fig. 6. Nyquist plots of the unmodified (●) and the modified (■) ASS N25 surfaces by applying 200 sweeps, recorded in a 0.16 M NaCl solution. Inset: Electric equivalent circuit used to fit experimental data.

Cyclic polarization of the surface of the steel results in an increase in the surface roughness, and thus in the real surface area exposed to the electrolyte. In order to eliminate the effect of surface area and determine the real general corrosion resistance, a true surface area was calculated for each sample. First, using

the Brug Equation[43] and CPE_1, the corresponding capacitance was calculated and presented in Table II. Taking into account that a double-layer capacitance of a smooth electrode surface is 25 μF cm^{-2},[44] the true surface area of each investigated ASS N25 sample was calculated as a ratio, $A_{true} = C_{DL}/25$ (cm^2), Table II. As can be seen, the electrochemical passivation of the surface resulted in a significant increase in the surface area, which is consistent with previous observations.[25] The numerical values of R_{true} were used to calculate the protection efficiency of the surface film according to the expression:

$$PE / \% = 100(R_{true,mod} - R_{true,unmod})/R_{true,mod} \quad (5)$$

where $R_{true,mod}$ and $R_{true,unmod}$ are the polarization resistance values of modified and unmodified samples, respectively. Table II shows that the electrochemical modification of the ASS N25 surface resulted in an increase in the general corrosion resistance, yielding a corrosion protection efficiency of *ca*. 90 %.

TABLE II. Impedance parameters for the ASS N25 electrode in a 0.16 M NaCl solution at the open circuit potential

Treatment	$Q_1 \times 10^6$ Ω^{-1} cm^{-2} s^n	n	R_1 kΩ cm^2	C_0 μF cm^{-2}	C_{dl} μF cm^{-2}	R_{true} kΩ cm^2
Unmodified	33.7	0.81	283	–	57	638
$Modified_{100}$	162.1	0.89	342	170	201	3491
$Modified_{200}$	144.0	0.90	356	780	234	4248

CONCLUSIONS

This work proves the applicability of the electrochemical cyclic polarization method for increasing the corrosion resistance of the surface film of ASS N25 steel.

The superior pitting resistance of the modified surface compared to the control surface was attributed to the modification of the electronic properties of the passive film, though conversion of the type of semiconductivity (from *n*- to *p*-type) in the pitting-susceptible region. This is due to the enrichment of the electrochemically formed passive film with Cr(VI) species (XPS), which results in a "replacement" of pitting-initiating oxygen vacancies by metal vacancies. The resulting oxide layer is a semiconductor of *p*-type and thus more corrosion resistant against pitting attack. The other beneficial consequence of the electrochemical passivity was an improvement in the general corrosion resistance of the surface.

LIST OF SYMBOLS

A area, cm^2
C capacitance, F cm^{-2}
C_0 faradaic pseudocapacitance, F cm^{-2}
CPE constant phase element
E potential, V
e charge of electron, 1.602×10^{-19} C

j current density, A cm^{-2}
k Boltzmann constant, 1.23 × 10^{-23} J K^{-1}
M metal
N charge carrier density, cm^{-3}
n exponent of the constant phase element
ox oxygen lattice site
PE protection efficiency, %
Q frequency-independent constant, (Ω^{-1} cm^{-2} s^{n})
R resistance, Ω cm^2
T temperature, K
V vacancy
Z impedance, Ω cm^2.

Greek letters

ε relative permittivity
ε_o vacuum permittivity, ε_o = 8.85×10^{-14} F cm^{-1}
● positive charge.

Sub/superscripts

A acceptor
a anodic
c cathodic
D donor
DL double layer
fb flat band
el electrolyte
im imaginary
M metal site
mod modified
O oxygen
OCP open circuit potential
real real
SC space charge
true true
unmod unmodified.

ИЗВОД

ПРОМЕНА *n*-ТИПА У *p*-ТИП ПРОВОДЉИВОСТИ ПОЛУПРОВОДНИЧКОГ ПАСИВНОГ ФИЛМА ФОРМИРАНОГ НА N-АУСТЕНИТНОМ ЧЕЛИКУ: ПОВЕЋАЊЕ ОТПОРНОСТИ ПРЕМА ПИТИНГ КОРОЗИЈИ

MIRJANA METIKOŠ-HUKOVIĆ[1], ZORAN GRUBAČ[2] и SASHA OMANOVIC[3]

[1]Department of Electrochemistry, Faculty of Chemical Engineering and Technology, University of Zagreb, P. O. Box 177, 10000 Zagreb, Croatia, [2]Department of General and Inorganic Chemistry, Faculty of Chemistry and Technology, University of Split, N. Tesle 10, 21000 Split, Croatia and [3]Department of Chemical Engineering, McGill University, 3610 University Street, Montreal, Quebec, Canada H3A 2B2

Електрохемијска модификација површине N-легираног аустенитног нерђајућег челика (ASS N25) успешно је изведена како би се побољшала баријерна својства пасивног филма у растворима које садрже хлоридне јоне. Хемијски састав, електронске и

баријерне особине површинског филма, пре и после електрохемијског третмана (пасивације), испитивани су користећи фотоелектронску спектроскопију X-зрака (XPS), спектроскопију електрохемијске импеданције (EIS) и Mott–Schottky анализу. Резултирајућа супериорна отпорност модификоване ASS N25 површине према питинг корозији приписана је променама електронских (полупроводничких) својстава површинског филма. Проводљивост пасивног филма у подручју потенцијала осетљивом на питинг мења се из *n*- у *p*-тип током цикличне потенциодинамичке поларизације.

(Примљено 21. новембра, ревидирано 24. новембра 2013)

REFERENCES

1. V. G. Gavriljuk, H. Berns, *High Nitrogen Steels Structure Properties, Manufacture, Application*, Springer-Verlag, Berlin, 1999
2. U. Kamachi Mudali, S. Ningshen, *Trans. Indian Inst. Met.* **55** (2002) 461
3. S. Ningshen, U. Kamachi Mudali, V. K. Mittal, H. S. Khatak, *Corros. Sci.* **49** (2007) 481
4. M. Metikoš-Huković, R. Babić, Z. Grubač, Ž. Petrović, N. Lajçi, *Corros. Sci.* **53** (2011) 2176
5. H. Baba, T. Kodama, Y. Katada, *Corros. Sci.* **44** (2002) 2393
6. F. M. Bayoumi, W. A. Ghanem, *Mater. Lett.* **59** (2005) 3311
7. D. Gopi, V. C. A. Prakash, L. Kavitha, S. Kannan, P. R. Bhalaji, E. Shinyjoy, J. M. F. Ferreira, *Corros. Sci.* **53** (2011) 2328
8. D. Gopi, J. Indira, L. Kavitha, *Surf. Coat. Tech.* **206** (2012) 2859
9. V. Maurice, P. Marcus, *Electrochim. Acta* **84** (2012) 129
10. H.-H. Strehblow, V. Maurice, P. Marcus, in: *Corrosion Mechanisms in Theory and Practice*, 3rd ed., P. Marcus, Ed., CRC Press, Taylor and Francis, Boca Raton, FL, 2011, p. 235
11. P. Marcus, V. Maurice, in: *Oxide Ultrathin Films, Science and Technology*, G. Pacchioni, S. Valeri, Eds., Wiley–VCH Verlag, Weinheim, Germany, 2012, p. 119
12. P. Marcus, H.-H. Strehblow, V. Maurice, *Corros. Sci.* **50** (2008) 2698
13. A. Seyeux, V. Maurice, P. Marcus, *Electrochem. Solid State Lett.* **12** (2009) C25
14. M. Bojinov, G. Fabricius, T. Laitinen, K. Mäkelä, T. Saario, G. Sundholm, *Electrochim. Acta* **45** (2000) 2029
15. S. Martinez, M. Metikoš-Huković, N. Lajci, *Passivity of Nitrogen-Bearing Stainless Steel in Acidic Solution*, in *Passivation of metals and semiconductors, and properties of thin oxide layers*, P. Marcus, V. Maurice, Eds., Elsevier, Amsterdam, 2006, p. 35
16. D. D. MacDonald, *J. Electrochem. Soc.* **139** (1992) 3434
17. D. D. MacDonald, S. R. Biaggio, H. Song, *J. Electrochem. Soc.* **139** (1992) 170
18. J. S. Noh, N. J. Laycock, W. Gao, D. B. Wells, *Corros. Sci.* **42** (2000) 2069
19. C.-C. Shih, C.-M. Shih, Y.-Y. Su, L. H. J. Su, M.-S. Chang, S.-J. Lin, *Corros. Sci.* **46** (2004) 427
20. G. T. Burstein, R. M. Souto, *J. Electrochem. Soc.* **151** (2004) B537
21. S. Fujimoto, T. Yamada, T. Shibata, *J. Electrochem. Soc.* **145** (1998) L79
22. T. M. Yue, J. K. Yu, H. C. Man, *Surf. Coat. Technol.* **137** (2001) 65
23. Z. Bou-Saleh, A. Shahryari, S. Omanovic, *Thin Solid Films* **515** (2007) 4727
24. A. Shahryari, S. Omanovic, J. A. Szpunar, *Mater. Sci. Eng., C* **28** (2008) 94
25. A. Shahryari, S. Omanovic, J. A. Szpunar, *J. Biomed. Mater. Res., A* **89** (2009) 1049
26. M. P. Ryan, D. E. Williams, R. J. Chater, B. M. Hutton, D. S. McPhail, *Nature* **415** (2002) 770

27. M. F. Montemor, A. M. P. Simões, M. G. S. Ferreira, M. Da Cunha Belo, *Corros. Sci.* **41** (1999) 17
28. M. Da Cunha Belo, B. Rondot, C. Compere, M. F. Montemor, A. M. P. Simões, M. G. S. Ferreira, *Corros. Sci.* **40** (1998) 481
29. M. Z. Yang, J. L. Luo, Q. Yang, L. J. Qiao, Z. Q. Qin, P. R. Norton, *J. Electrochem. Soc.* **146** (1999) 2107
30. Y. F. Cheng, J. L. Lou, *Electrochim. Acta* **44** (1999) 2947
31. S. R. Morrison, *Electrochemistry at Semiconductor and Oxidised Metal Electrodes*, Plenum Press, New York, 1980
32. R. Babić, M. Metikoš-Huković, *J. Electroanal. Chem.* **358** (1993) 143
33. M. Bojinov, G. Fabricius, T. Laitinen, K. Makela, T. Saario, G. Sundholm, *Electrochim. Acta* **46** (2001) 1339
34. T. L. Sudesh, L. Wijesinghe, D. J. Blackwood, *Corros. Sci.* **50** (2008) 23
35. F. Gaben, B. Vuillemin, R. Oltra, *J. Electrochem. Soc.* **151** (2004) B595
36. Y. X. Qiao, Y. G. Zheng, W. Ke, P. C. Okafor, *Corros. Sci*. **51** (2009) 979
37. A. Fattah-Alhosseini, M. A. Golozar, A. Saatchi, K. Raeissi, *Corros. Sci.* **52** (2010) 205
38. K. S. Raja, D. A. Jones, *Corros. Sci*. **48** (2006) 1623
39. B. A. Boukamp, *Equivalent circuit users manual*; report CT88/265/128, University of Twente, Twente, 1989, p. 13
40. M. Metikoš-Huković, Z. Grubač, R. Babić, N. Radić, *Corros. Sci.* **52** (2010) 352
41. M. Bojinov, I. Kanazirski, A. Girginov, *Electrochim. Acta*, **41** (1996) 2695
42. M. Metikoš-Huković, Z. Grubač, *J. Electranal. Chem*. **556** (2003) 167
43. G. J. Brug, A. L. G. van der Eeden, M. Sluyters-Rehbach, J. H. Sluyters, *J. Electroanal. Chem.* **176** (1984) 275
44. L. Chen, A. Lasia, *J. Electrochem. Soc.* **139** (1992) 3214.